

## RICA - Radio Imaging Combination Analyzer

1 MILES LUCAS<sup>1,2</sup>

2 <sup>1</sup>*Iowa State University, Ames, Iowa*

3 <sup>2</sup>*National Radio Astronomy Observatory, Socorro, New Mexico*

### 4 ABSTRACT

### 5 1. INTRODUCTION

6 In radio synthesis imaging a common problem arising from interferometry is the lack of zero-spacing  
7 data. Without this data, images lack total power information. Single dish radio telescopes retain  
8 this total power information but lack the angular resolution capabilities of radio interferometers. To  
9 solve this problem, astronomers combine the interferometry data with the total power data. This  
10 report seeks to characterize the effectiveness of different combination methods and parameters.

11 The parameters analyzed were multiscale deconvolution versus normal Hogbom deconvolution, the  
12 effect of single-dish size on the combination, masking, and number of total iterations (i.e. depth of  
13 clean). One of the previous assumptions is that if the single-dish UV-coverage does not adequately  
14 complement the interferometer UV-coverage, feathering will not be effective. Another assumption is  
15 that simple point structures should not see much discrepancy in parameters or methods. Multiscale  
16 deconvolution is supposed to help pick up fluffy structure better due to its multi-pass method of  
17 creating model images in the Cotton-Schwab Cycle, as opposed to Hogbom's  $\delta$ -function method.  
18 Therefore, more complex, fluffy structure ought to show more distinction in results.

19 There are four methods of combination that were tested. The first is CASA's *feather* task. The  
20 process of feathering starts with regridding the lower resolution to the higher resolution image. Each  
21 is then Fourier transformed and gridded, while the lower resolution data is scaled by the ratio of the  
22 clean beams (high resolution/low resolution). The high-resolution grid is then added to this, scaled

23 by a weighting that starts at 0 and increases to 1 as the wavelength increases. This final combination  
 24 is then inverse Fourier transformed back into the image plane.

25 The next method is using the total power image as the starting model in CASA’s *tclean* task. In  
 26 the Cotton-Schwab CLEAN algorithm (CSCLEAN), each major-cycle begins with a blank model  
 27 image and constructs an image on it by using minor-cycle iterations. By using a starting model,  
 28 this model is no longer blank, but is passed as a parameter. By using the total power image as the  
 29 starting model, we can hope to retain the total power information through the CLEAN algorithm.

30 Another modification to the Cotton-Schwab cycle in order to combine images is by doing a modi-  
 31 fied joint deconvolution. In each major Cotton-Schwab cycle, the visibilities are gridded and inverse  
 32 Fourier transformed to create an image residual, which is then feathered with the total power residual  
 33 before deconvolving. The deconvolved model is then convolved with the single-dish beam and sub-  
 34 tracted from the previous single-dish residual. The deconvolved model is also Fourier transformed,  
 35 degridded, and subtracted from the visibilities to create a new residual image. These residuals are  
 36 then degridded and transformed to finish the major cycle. See [Figure 1](#) for a visual flowchart of the  
 37 process.

38 The last method of combination we use is *tp2vis*, which takes the total power image and spoofs a  
 39 measurement set. The way *tp2vis* accomplishes this is by taking Fourier data from the total power  
 40 image and sparsely sampling the Fourier data at close spacings (see [Koda et al. 2011](#)). This data  
 41 can be concatenated with the interferometer data and deconvolved in *tclean*. [Figure 2](#) shows how  
 42 the single-dish is simulated and concatenated with the interferometer data. This should help fill  
 43 the close-spacing gap created by the interferometer data and subsequently help increase total power  
 44 information.

## 45 2. METHODS

46 In order to evaluate the different combination methods, a metric needed to be created and tested  
 47 on a suite of models. The metrics used were CLEAN residuals, fidelity images, and a ratio of the  
 48 power spectrum densities (PSD). The fidelities are given [Equation 1](#)

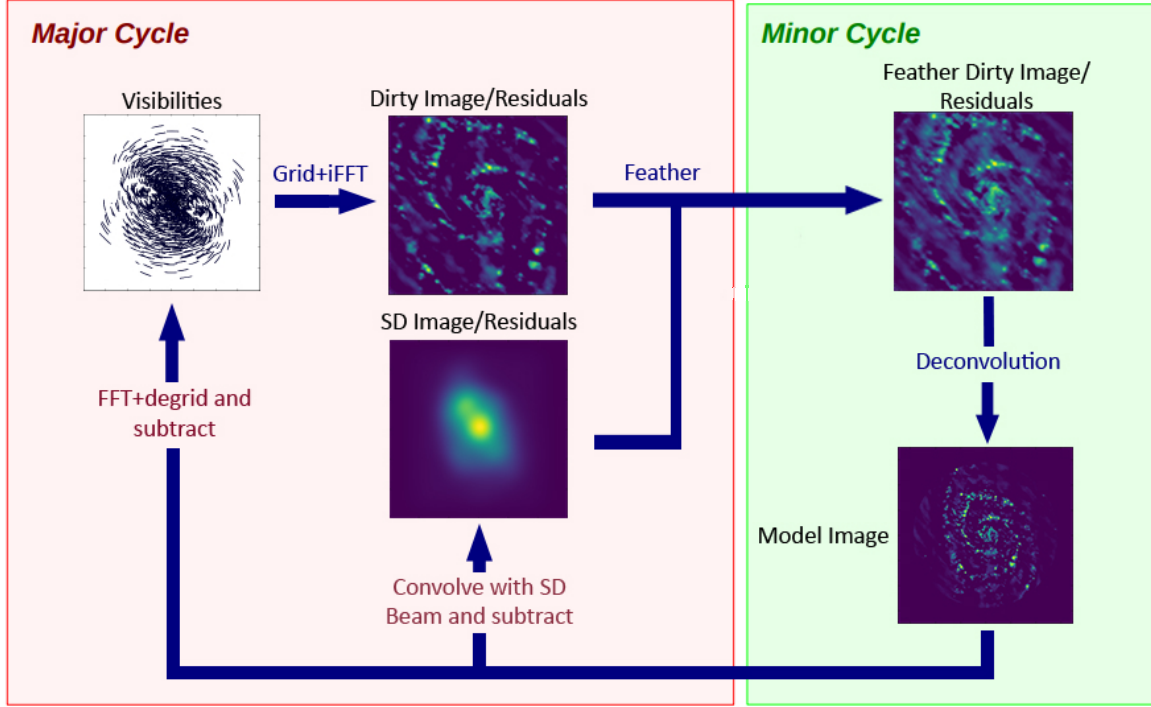


**Figure 1.** A flow chart describing the joint-deconvolution approach to combining interferometer and single dish data. Adapted from Rau, U. & Naik, N. 2018 (in prep).

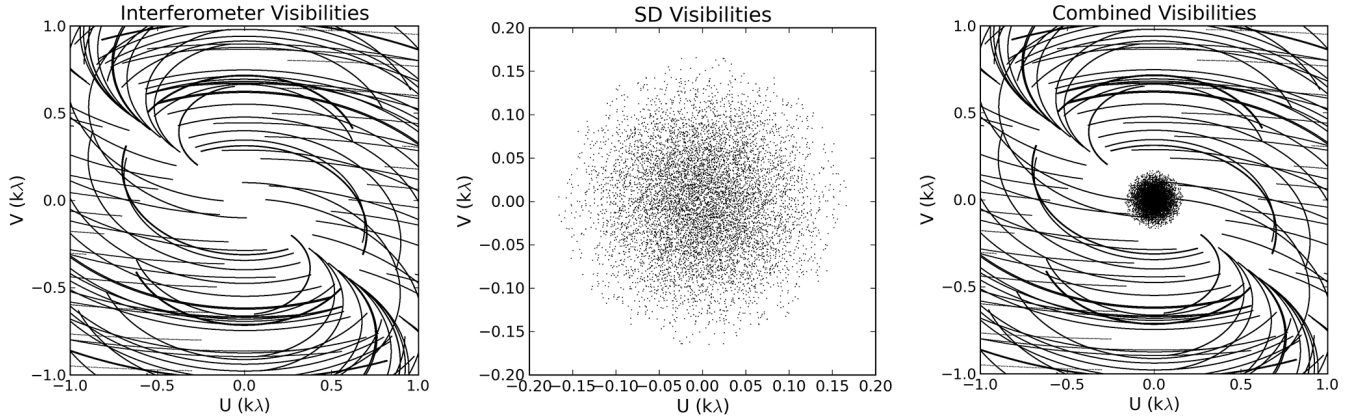


**Figure 2.** A look at how the visibilities are added through using tp2vis for a model simulated on the VLA A configuration. In the center of the interferometer image in the first plot shows sparsity that is filled in on the third plot. The second plot shows the approximation tp2vis makes of the single dish.

$$\text{Fidelity}(i, j) = \frac{|\text{Model}(i, j)|}{\max(|\text{Difference}(i, j)|, 0.7 \times \text{rms}(\text{Difference}))} \quad (1)$$

49 where model is the reference image and diff is the difference between the test and reference images  
 50 (Pety et al. 2011, p.19). The exigence for using PSDs is that the zero-spacing power is readily visible  
 51 for every image. By using these ratios, the closer the ratio is to 1.0 at short spacings (when compared  
 52 to the true model), the more accurate the combination. In addition, when compared with the total  
 53 power image, it shows how much effective weight is given to the total power image in the combination.  
 54 The ratio of the PSDs is given by Equation 2

$$\text{Ratio}(UV) = \frac{\text{Power}_{test}(UV)}{\text{Power}_{ref}(UV)} \cdot \frac{\text{BA}_{ref}}{\text{BA}_{test}} \quad (2)$$

$$\text{err}(UV) = \left( \frac{\text{Power}_{ref}(UV) + \text{Power}_{test}(UV)}{2} \right)^{-1} \quad (3)$$

55 where Power is the power from the PSD, BA is the beam area, *ref* refers to the reference image  
 56 (model or SD), and *test* refers to whichever image is being tested. The uncertainty given is Equation 3  
 57 such that the uncertainty is the reciprocal of the average of the PSDs.

58 Each combination was compared to both the true model and the single dish, total power image.  
 59 Many models were tested with various extra parameters. Three models were generated from com-  
 60 ponent lists. One has 4 point sources, one has a single Gaussian source, and one has a mixture of 4  
 61 point sources, one very broad Gaussian, and one off-center, stronger Gaussian. There were also various  
 62 models based off real structure, including M51 (based off an H- $\alpha$  image), Orion, RXJ1347, and a  
 63 protoplanetary disk (PPD) simulation. Figure 3 shows all of the models. It is important to note  
 64 that these models have been regridded onto a common coordinate system that is not representative  
 65 of the true astronomical targets. This was in effort to simplify the simulation process for creating  
 66 measurement sets.

67 The code base for testing the effectiveness is hosted publicly for anyone to use<sup>1</sup>. In the source code  
 68 there are many scripts and methods to facilitate simulating, combining, and comparing. Every model

<sup>1</sup> <https://gitlab.com/mileslucas/rica>

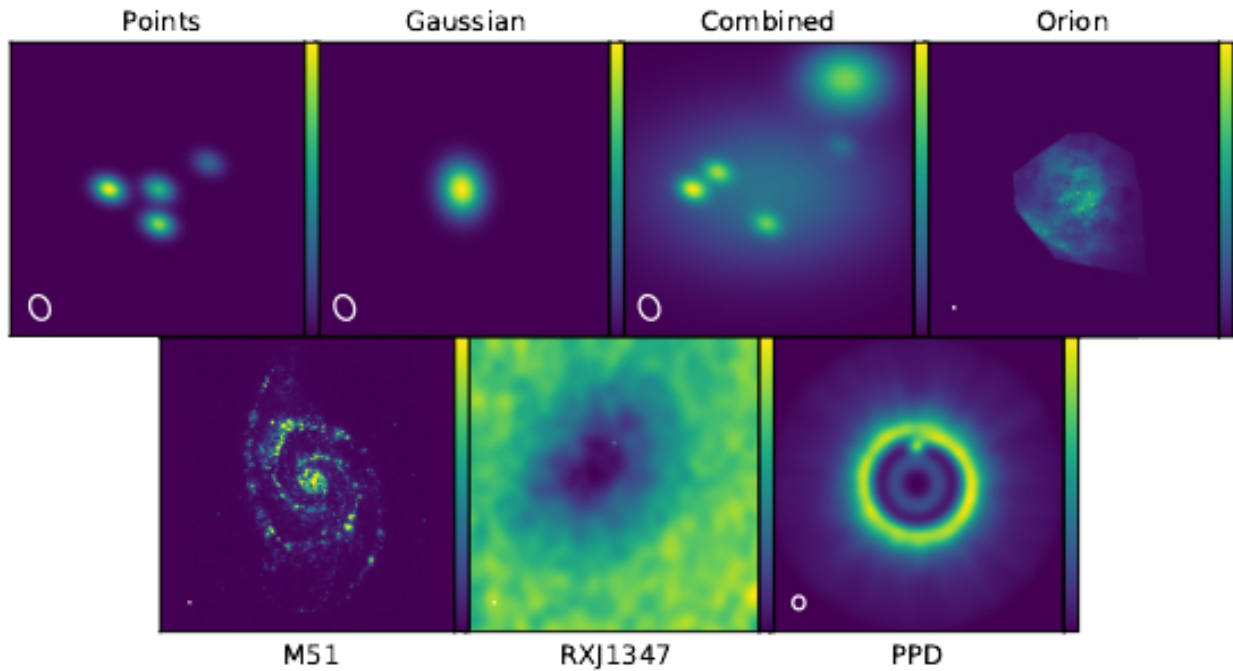


**Figure 3.** The models used for testing combination methods convolved with some restoring beam to show structure better.

is described in `src/_models.py` with a dictionary defining the simulation and `tclean` parameters. The pipeline for testing these models was as follows:

1. Simulate measurement set (MS) based on VLA configurations
2. Simulate single dish image by convolving model with Gaussian
3. Image the MS
4. Do the combinations (feather, startmodel, joint deconvolution, and `tp2vis`)
5. For each combination, do a comparison with the true model (convolved with the restoring beam) and the single dish image

and is implemented in `src/pipeline.py`.

### 2.1. *Simulations and Deconvolution*

All simulations were done using the VLA for the telescope model except for the PPD simulation, which was done using `simalma` and was only simulated once. Each test model could define which

81 of the VLA configurations to use, from A, B, BnA, C, CnB, D, and DnC. The spectral window for  
 82 the simulations mimic the VLA C-band at 4.5 GHz to 5.5 GHz (central 5 GHz) with 101 channels at  
 83 10 MHz intervals. The field observed was J2000 21h28m31.0 45°0'0.0''. The observation date and  
 84 time was 2018/06/01 at 12:00:00.0 UTC. The integration time was 10 s each with a total of 30 000 s.  
 85 Finally, the data was corrupted with 1 mJy of simple noise.

86 The single dish images were created by taking the true model and convolving with a Gaussian  
 87 equivalent to the single dish beam at the given frequency.

$$\text{FWHM}(\nu, D) = \frac{3.66 \times 10^8 \text{ m s}^{-1}}{\nu \cdot D} \quad (4)$$

88 Equation 4 gives the Gaussian kernel full-width half-maximum (FWHM) in radians for a frequency  
 89 in Hz and dish diameter in meters. For instance, to simulate data from the Green Bank Telescope  
 90 (GBT) with a dish diameter of 100 m at 5 GHz gives a FWHM of 2'31'', which is in agreeance with  
 91 values from the GBT proposer's guide<sup>2</sup>. Note that this is not the most accurate equation for other  
 92 telescopes, because there is a constant involved in this equation based off the taper-length of the  
 93 telescope's feedhorns. In addition, these single dish images have  $5 \times 10^{-6}$  uniform noise added.

94 Each model defines its own parameters for cleaning. Appendix A lists every single parameter for  
 95 each model. As a default, a model simulated in VLA D configuration has an image size of 64 with  
 96 a cell size of 7.0''. The restoring beam for the D configuration is approximately 20.41'' by 15.60'' so  
 97 the cell accounts for half to a third of the beam width. In general, cleaning was done with very high  
 98 numbers of iterations, relying on a threshold to stop the algorithm for consistency. This differs for  
 99 the models tested at explicitly different cleaned levels.

## 100 2.2. Comparisons

101 Each comparison was ran with the same clean parameters for consistency. Because *feather* does  
 102 not actively clean, it has its own set of parameters, but all of the models tested used the default  
 103 parameters. After all the combination permutations were imaged, they were compared against the

<sup>2</sup> p.9, <https://science.nrao.edu/facilities/gbt/proposing/GBTpg.pdf>

104 true model convolved with the restoring beam and the single dish image alongside the uncombined  
 105 interferometer image. All of the ratio were saved into individual CSV files for further analysis. In  
 106 all, each model has 10 comparisons (5 against the models and 5 against the single-dish images) and  
 107 4 separate cleans to perform.

108 In order to run a new model to test comparison methods, there are two general methods. If there  
 109 exists a true model, simply add an entry to the models dictionary defining the simulation and clean  
 110 parameters. It is also important to edit *src/simulate.py* to accommodate the new model. Follow the  
 111 existing code base for guidance. It is also important to create a copy of the model and regrid it to  
 112 the common coordinate system (use an existing model to retrieve the coordinate system). The model  
 113 can then be ran through the pipeline along with any other models using *src/pipeline.py*.

114 If there is no true model, it is still useful to test and compare against the total power image, alone. In  
 115 this case, using a cleaned image, a measurement set, and a total power image with the *src/combine.py*  
 116 script will produce all of the combinations. These can then be compared using *src/compare.py*. It is  
 117 possible to edit *src/pipeline.py* to accommodate special models, see how the PPD model is handled  
 118 in the pipeline.

### 119 3. RESULTS

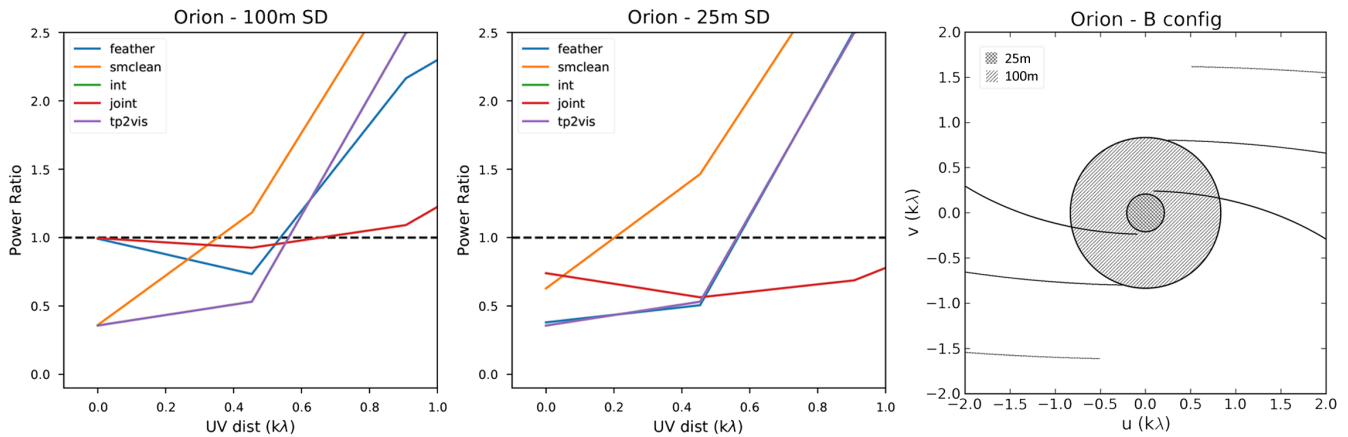


**Figure 4.** The left two plots are ratios for each combination method between two different single dish sizes. The horizontal line marks the ideal ratio for close UV spacing. The right plot shows the UV coverage of the interferometer with the coverage of the 100 m and 25 m single dishes overlaid.

120 For fidelity images and ratios of every comparison, see Appendix B. This section will only comment  
 121 on a few models and comparison highlighting trends. The effect of single dish size was apparent on  
 122 the accuracy of combinations. Figure 4 shows how the ratios compare between the 100 m single dish  
 123 size for the Orion model in B configuration and the 25 m single dish size of the same model. Notably,  
 124 *feather* does not work as well for small single dish sizes. Both start model and joint deconvolution  
 125 combination methods are able to do better than the plain interferometer with the small dish, but  
 126 still do not reach that ideal ratio that is possible for the larger single dish. Looking at the coverage  
 127 of the single dishes, the 25 m dish does not overlap with the interferometer data at all.

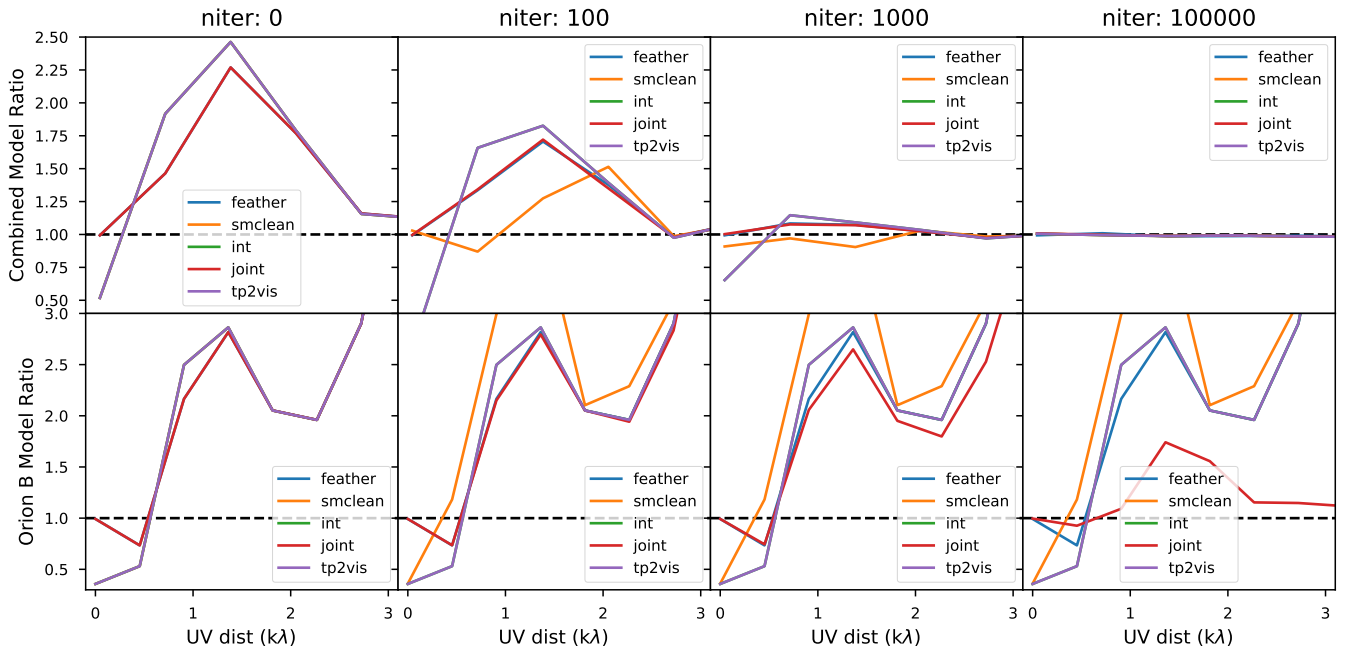


**Figure 5.** A comparison showing the effect on the combinations due to the depth of cleaning for two models, ‘combined’ and ‘orion-b’. The dashed black line represents the ideal ratio for the true model comparison.

128 Next, Figure 5 shows the effect that depth of cleaning has on the power ratios. Each row corre-  
 129 sponds to each model and each column is a depth of cleaning based on the number of iterations of  
 130 deconvolution. The ‘combined’ model is a much simpler model than the ‘orion-b’ model. First, the  
 131 joint deconvolution worked well regardless of the depth of cleaning for both models. Even completely  
 132 dirty images had great total power information. After some amount of cleaning, *feather* quickly rose

133 to the same level as joint deconvolution and in the ‘combined’ model, using a start model started  
 134 working after some cleaning. In the simpler, ‘combined’ model, all combination methods converged  
 135 at high enough iterations- even the interferometer image. However, for the more complex, ‘orion-b’  
 136 model, start model never converged and the values of the ratios remained erratic even at full cleaning  
 137 depth.

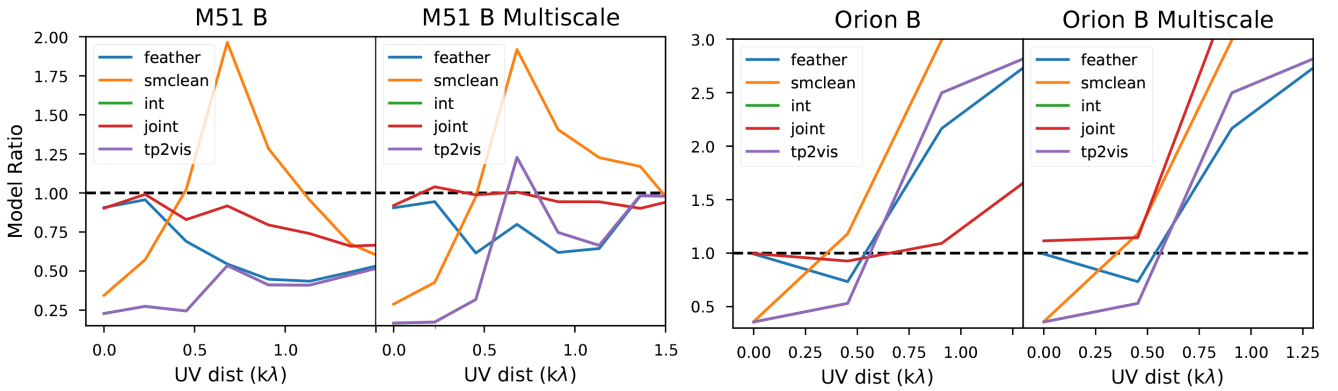


**Figure 6.** A comparison showing the effect on the combinations due to multiscale deconvolution for two models, ‘m51-b’ and ‘orion-b’. The dashed black line represents the ideal ratio for the true model comparison.

138 Figure 6 shows how multiscale deconvolution affects the combinations. For each model, there are  
 139 some slight variations, but in general the ratios stay consistent. The ‘orion-b’ multiscale model does  
 140 show a weird overshoot in the power for the joint deconvolution which does not show up in any other  
 141 ‘orion-b’ models.

#### 4. CONCLUSION

143 From the results of the single dish sizes, the main factor in algorithm success is the amount of  
 144 overlap of the single dish and interferometer data. This could be the reason why feather fails so  
 145 much and why joint deconvolution and start model are not quite as good, either. Future studies  
 146 might find the point at which there is enough overlay for each method to “succeed”.

147 In regards to the depth of cleaning, in general, more is better. Joint deconvolution seemed to work  
 148 for any dirty image with enough single dish coverage, but for future studies, it would be nice to try  
 149 and see if joint deconvolution works for dirty images of many more models. In conjunction with the

150 study on single dish size, there were no combinations that retrieved the total power information well  
 151 from the dirty image due to insufficient single dish coverage<sup>3</sup>

152 The multiscale analysis shows that there really is not much effect from using multiscale cleaning.  
 153 There could be more testing done by using different scales and using different models that may lend  
 154 more towards multiscale's favor with very complex, intricate structures.

155 Thank you to Dr. Kumar Golap and Dr. Takahiro Tsutsumi for their guidance and assistance.  
 156 This work was funded by the National Science Foundation in partnership with the National Radio  
 157 Astronomy Observatory and Associated Universities Incorporated.

158 *Software:* [CASA](#), [tp2vis](#) ([Koda et al. 2011](#))

## REFERENCES

- |  |
|--|
| <p>159 Koda, J., Sawada, T., Wright, M. C. H., et al.      162 Pety, J., Gueth, F., &amp; Guilloteau, S. 2011, ALMA<br/>   160 2011, ApJS, 193, 19,    163 Memo #398 Impact of ACA on the Wide-Field<br/>   161 doi: <a href="https://doi.org/10.1088/0067-0049/193/1/19">10.1088/0067-0049/193/1/19</a>                                    164 Imaging Capabilities of ALMA, Tech. rep.</p> |
|--|

<sup>3</sup> see 'orion-b-25-n0' ratio data

165

## APPENDIX

166

### A. MODEL PARAMETERS

167

168

169

The following table describes the parameters used for cleaning the model images. The only exception is the model ‘combined-sp’, which additionally uses specmode=’cube’ and nchan=-1 to facilitate cube imaging. For more details, look at the *src/\_models.py* file, which this table is generated from.

**Table 1.** The parameters for every model ran through the pipeline

Name	Model	Config	SD size	imsize	cell	niter	cycleniter	threshold	deconvolver	scales	mask
points	points	VLA d	100 m	[64, 64]	7.00arcsec	100000	100	1e-5Jy	hogbom	No	
gauss	gauss	VLA d	100 m	[64, 64]	7.00arcsec	100000	100	1e-5Jy	hogbom	No	
combined	combined	VLA d	100 m	[64, 64]	7.00arcsec	100000	100	1e-5Jy	hogbom	No	
combined-n0	combined	VLA d	100 m	[64, 64]	7.00arcsec	0	100	1e-5Jy	hogbom	No	
combined-n100	combined	VLA d	100 m	[64, 64]	7.00arcsec	100	100	1e-5Jy	hogbom	No	
combined-n1000	combined	VLA d	100 m	[64, 64]	7.00arcsec	1000	100	1e-5Jy	hogbom	No	
combined-ms	combined	VLA d	100 m	[64, 64]	7.00arcsec	100000	100	1e-5Jy	multiscale	[0, 3, 10, 30]	
m51	m51	VLA d	100 m	[128, 128]	7.00arcsec	100000	100	1e-12Jy	hogbom	No	
m51-ms	m51	VLA d	100 m	[128, 128]	7.00arcsec	100000	100	1e-12Jy	multiscale	[0, 3, 10, 30]	
m51-b	m51	VLA b	100 m	[1400, 1400]	0.65arcsec	100000	100	1e-12Jy	hogbom	No	
m51-b-ms	m51	VLA b	100 m	[1400, 1400]	0.65arcsec	100000	100	1e-12Jy	multiscale	[0, 3, 10, 30]	
orion-b	orion	VLA b	100 m	[700, 700]	0.65arcsec	100000	400	1e-9Jy	hogbom	Yes	
orion-b-n0	orion	VLA b	100 m	[700, 700]	0.65arcsec	0	100	1e-9Jy	hogbom	Yes	
orion-b-n100	orion	VLA b	100 m	[700, 700]	0.65arcsec	100	100	1e-9Jy	hogbom	Yes	

*Table 1 continued on next page*

**Table 1** (*continued*)

Name	Model	Config	SD size	imsize	cell	niter	cycleniter	threshold	deconvolver	scales	mask
orion-b-n1000	orion	VLA b	100 m	[700, 700]	0.65arcsec	1000	100	1e-9Jy	hogbom	Yes	
orion-b-ms	orion	VLA b	100 m	[700, 700]	0.65arcsec	100000	400	1e-9Jy	multiscale	[0, 3, 10, 50]	
orion-b-25	orion	VLA b	25 m	[700, 700]	0.65arcsec	100000	400	1e-9Jy	hogbom	Yes	
orion-b-25-n0	orion	VLA b	25 m	[700, 700]	0.65arcsec	0	100	1e-9Jy	hogbom	Yes	
orion-b-25-n100	orion	VLA b	25 m	[700, 700]	0.65arcsec	100	100	1e-9Jy	hogbom	Yes	
orion-b-25-n1000	orion	VLA b	25 m	[700, 700]	0.65arcsec	1000	100	1e-9Jy	hogbom	Yes	
orion-b-25-ms	orion	VLA b	25 m	[700, 700]	0.65arcsec	100000	400	1e-9Jy	multiscale	[0, 3, 10, 30]	
orion-c	orion	VLA c	100 m	[216, 216]	2.12arcsec	100000	400	1e-9Jy	hogbom	No	
RXJ1347	RXJ1347	VLA a	100 m	[2268, 2268]	0.20arcsec	100000	100	1e-6Jy	hogbom	No	
RXJ1347-masked	RXJ1347	VLA a	100 m	[2268, 2268]	0.20arcsec	100000	100	1e-6Jy	hogbom	Yes	
ppd	ppd	ALMA	ACA	[192, 192]	0.01arcsec	100000	100	1e-7Jy	hogbom	No	

170

## B. MODEL RESULTS

171 For data tables of every single comparison, visit the [RICA repository](#).

172 **Fig. Set 1. Model Results**

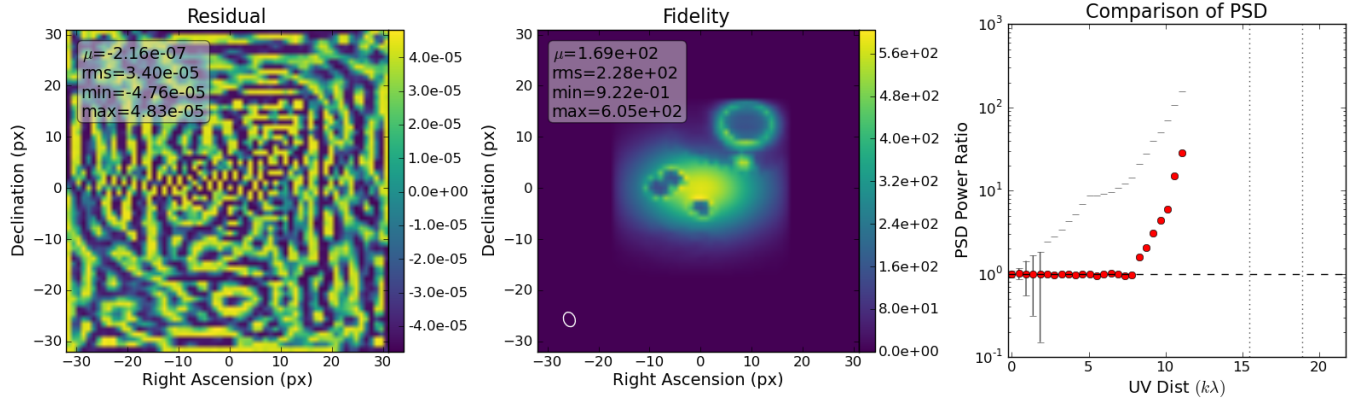


**Figure 7.** Comparison of feather combination to the true model for combined simulation. The ratio is Equation 2. The black ticks are error bars on a scaled uncertainty based on Equation 3. The vertical lines are the maximum UV distance of the interferometer at the longest and shortest wavelengths, respectively. The complete figure set (125 figures) is available at the [RICA repository](#).